Research Square

Preprints are preliminary reports that have not undergone peer review.
They should not be considered conclusive, used to inform clinical practice,
or referenced by the media as validated information.

PeriCont: continuation of relative periodic orbits of the planar equal-mass three-body problem through close two-body approaches

Utshob Kandel

utshobkandel@gmail.com

Unaffiliated https://orcid.org/0009-0008-3981-0859

Research Article

Keywords: three-body problem, relative periodic orbits, continuation, regularization, close approaches, multiple precision

Posted Date: November 18th, 2026

DOI: https://doi.org/10.21203/rs.3.rs-11737991/v1

License: This work is licensed under a Creative Commons Attribution 4.0 International License.
Read Full License

Additional Declarations: The authors declare no competing interests.

PeriCont: continuation of relative periodic orbits of the planar equal-mass three-body problem through close two-body approaches

Utshob Kandel[a,*]

[a] *Unaffiliated, Chitwan, Nepal*

Abstract

Continuation of families of relative periodic orbits of the planar equal-mass three-body problem breaks down where two bodies pass close. PeriCont follows families through such passes: multiple shooting with 24 pieces, pseudo-arclength continuation, IAS15 for the pieces and, for a piece with a close pair, algorithmic regularisation with a derivative at a fixed time worked out by hand. Stored points are checked in 40 or 50 digits by separate code. The regularised integrator makes the difference: with IAS15 alone or Dormand–Prince alone the corrector fails on these stretches. Four families reach checked pair distances of 7.3e-10 to 1.6e-8 (where the steps landed); collision orbits are bracketed by a sign change of the pair's angular momentum. On the stretches tested PeriCont is not cheaper per unit of λ than a 50-digit natural continuation; it gives a double-precision trace through the close approaches, which passes folds in λ. Three traces stall at a double-precision floor of the residual, which the hand-over to the 50-digit continuation passes on the two traces where it was run. Two traces go on past their guard when it is only recorded. Hénon's family m, closed again in 50 digits, agrees with his printed 8 digits.

Keywords: three-body problem, relative periodic orbits, continuation, regularisation, shooting, close approaches, multiple precision

PROGRAM SUMMARY

Program title: PeriCont, version 0.3.0 (tag date 2026-11-02)

*Corresponding author. E-mail: utshobkandel@gmail.com

CPC Library link to program files: (to be added by Technical Editor)
Developer's repository link: `https://github.com/Utshob-k/orbit-hunter` (tag `v0.3.0`, branch `release-0.3`)
Licensing provisions: MIT license (MIT) for the code; the data, the documents and the README, which are the supplementary material, are under CC BY 4.0
Programming language: JavaScript (Node.js 24.15) and Python 3.14 (REBOUND 5.2.2, mpmath 1.4.1, numpy 2.5.3)
Supplementary material: the data of `data/deep` in the package (traces, checks, re-closed stretches, and the results behind the tables) and the raw files on Zenodo, `https://doi.org/10.5281/zenodo.23864862`
Nature of problem: Relative periodic orbits of the planar problem of three bodies of equal mass form one-parameter families. A family is followed by continuation, which needs the flow over a period and its derivative. Where two bodies pass at a small distance the flow is badly conditioned, and an integrator without regularisation gives an end state whose error is far above the tolerance of the corrector. A result in double precision also needs an independent check, because the instability of an orbit amplifies rounding errors. PeriCont follows stretches of the families of orbits with a perpendicular start (three bodies on a line, all velocities perpendicular to it) through approaches of two bodies to pair distances of 7.3e-10, and gives each stored point an independent multiple-precision closure and smallest pair distance. Where the double-precision corrector stalls it can hand over to a 50-digit continuation.
Solution method: The half orbit is cut into 24 pieces (multiple shooting), and the family is followed by pseudo-arclength continuation with a Newton corrector. IAS15 in REBOUND (Rein and Spiegel, 2015; Rein and Liu, 2012) gives the end state of every piece. A piece whose smallest sampled pair distance is below 1e-3 is recomputed by a regularised integrator written for PeriCont: algorithmic regularisation in chain coordinates (Mikkola and Tanikawa, 1999; Preto and Tremaine, 1999), Bulirsch–Stoer extrapolation, a bracketed search for the end time, and a 12×12 derivative at a fixed physical time worked out by hand. Cross-checks, a check for missed flags and four guards protect the pieces. Stored points are checked by a multiple-precision flow (mpmath; Johansson and the mpmath development team, 2026) that shares no code with the integrators, and a re-closer closes selected orbits again in 50 digits. An optional hand-over continues a stalled trace in 50 digits.
Additional comments including Restrictions and Unusual features:

The corrector is for the planar problem, equal masses and the perpendicular start; the regularised integrator takes any masses for two or three bodies. It treats one close pair with the third body away from it, and the guards stop a trace when that is not so; with the guards only recorded, two traces go on past their stop (Section 4.3), and near a triple collision the method is untested. A user must supply a start orbit (u_1, u_2, λ, t); the repository finds such orbits with its Dormand–Prince route. The route was run with Node.js v24.15.0 and Python 3.14 only (Python 3.15 does not build REBOUND 5.2.2); the minimum supported versions are not established. The package holds 208 files (2.0 MB); its tests give 46 and 135 PASS lines, and a numeric sample run compares numbers with tolerances. The limits are in Section 8.

References:

- Mikkola, S., Tanikawa, K. (1999). Algorithmic regularization of the few-body problem. Monthly Notices of the Royal Astronomical Society 310, 745–749, https://doi.org/10.1046/j.1365-8711.1999.02982.x.
- Preto, M., Tremaine, S. (1999). A class of symplectic integrators with adaptive time step for separable Hamiltonian systems. The Astronomical Journal 118, 2532–2541, https://doi.org/10.1086/301102.
- Rein, H., Liu, S.-F. (2012). REBOUND: an open-source multi-purpose N-body code for collisional dynamics. Astronomy and Astrophysics 537, A128, https://doi.org/10.1051/0004-6361/201118085.
- Rein, H., Spiegel, D. S. (2015). IAS15: a fast, adaptive, high-order integrator for gravitational dynamics, accurate to machine precision over a billion orbits. Monthly Notices of the Royal Astronomical Society 446, 1424–1437, https://doi.org/10.1093/mnras/stu2164.

1. Introduction

1.1. The problem and the terms

Three bodies of equal mass attract each other by Newton's law and move in a plane. Orbits that return to their start after one period apart from a rotation of the whole configuration are relative periodic orbits; they occur in one-parameter families, followed by continuation: from one orbit the next is found by a Newton iteration that needs the flow over a period and its derivative. It is hardest where a family passes close to a collision orbit (an

orbit in which two bodies collide): an error before a close passage grows after it, and the derivative loses accuracy.

The orbits followed here have the perpendicular start (Figure 1). At time 0 the three bodies are on a line: body 1 at $x = -1$, body 2 at $x = \lambda$ and body 3 at $x = 1$, with velocities along y equal to u_1, u_2 and $-u_1 - u_2$. The code moves the centre of mass to the origin, which shifts x by $-\lambda/3$; Figure 1 is in that frame. The time t at which the bodies are on a line again with all velocities perpendicular to it is half the period. A family is a curve of such orbits in (u_1, u_2, λ, t); families are named as in the repository (t35 −; the sign is the direction of the trace in λ).

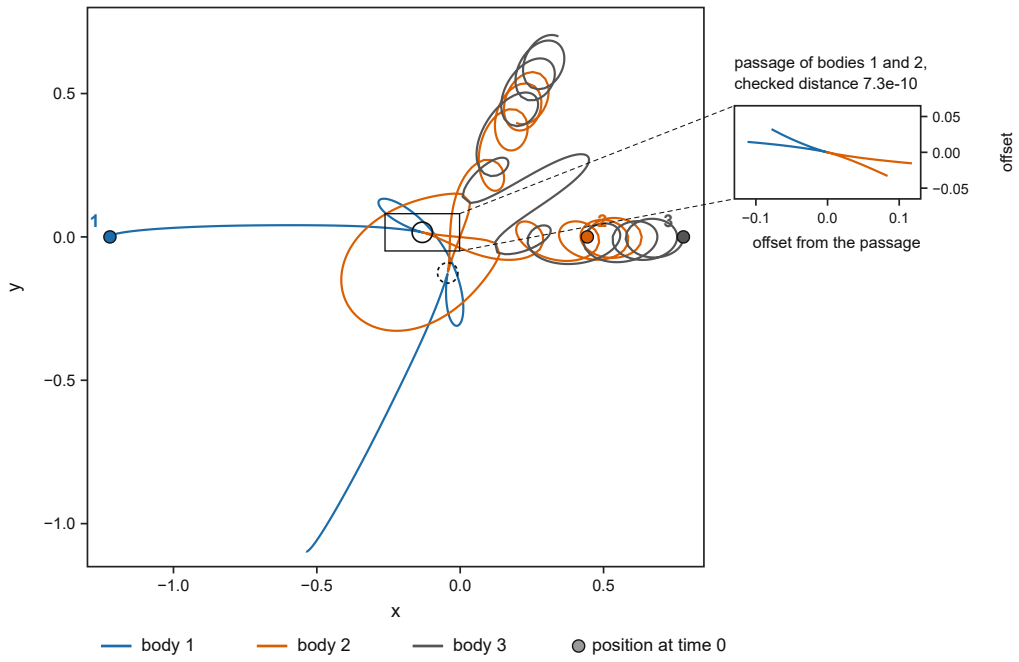


Figure 1: The orbit of t35 − at step 10 ($\lambda = 0.66485, T^* = 28.70$) over one period, in the frame of the code; it does not close, because the picture rotates by 1.1 rad. Inset: the tracks of the two bodies that pass at a pair distance of 8.7e-10, relative to the passage point, 0.03 in time on each side of the first passage.

Terms. A *step* is accepted when the corrector converges; steps are numbered by the attempt at which they were accepted, so "step 10" differs from "the 10th accepted step". A piece of the half orbit is an *encounter piece* if its smallest sampled pair distance is below 1e-3. A *check* of a stored point

is the integration of its start values over a full period in 40 or 50 digits by code that shares nothing with the integrators; it gives the closure of the orbit and its smallest pair distance, the *checked distance*. The *stall* of a trace is the stretch in which the corrector reaches its tolerance only at ever smaller steps in λ (Section 5.1); the *residual floor* is the smallest residual that double precision can resolve. A *hand-over* is the change from the double-precision corrector to a 50-digit continuation.

1.2. Earlier work

Hénon (1974) followed families of periodic orbits of the planar three-body problem by a differential correction in which Bulirsch–Stoer extrapolation with Waldvogel's regularisation integrated the orbit and the matrix came from finite increments of 1e-7; his masses were not equal; it is the nearest older method we found. Hénon (1976) followed the family m of equal masses from the collision orbit of Schubart (1956) and printed its orbits to 8 decimals, with a relation between period and rotation (Hénon, 1977 for the proof). Other continuation work is listed in Section 9.

1.3. What PeriCont adds

PeriCont is the close-approach route of the repository `github.com/Utshob-k/orbit-hunter`, version 0.3.0. Its parts exist separately in the sources we checked: Bulirsch–Stoer extrapolation of a regularised integration inside a Newton-type correction of relative periodic orbits of the planar three-body problem, with the matrix by finite differences (Hénon, 1974); multiple shooting with tangential continuation through a close approach, without regularisation (Wulff and Schebesch, 2008); pseudo-arclength continuation in multiple precision with a Taylor-series integrator, a double-precision family with selected orbits corrected to 100 digits afterwards (Dena et al., 2012); algorithmic regularisation with Bulirsch–Stoer extrapolation in a few-body code (Trani et al., 2019). We did not find in them a corrector whose matrix is the derivative, made by hand, of the regularised and extrapolated map, with the dependence on the end time removed by the implicit-function correction at the converged end, used in multiple shooting with pseudo-arclength continuation of relative periodic orbits of the three-body problem to pair distances of 7.3e-10, nor the checking of every stored point of a double-precision trace by a multiple-precision flow of a separate code that gives its closure and its smallest pair distance. The search covered 19 papers, not all there are.

2. Method

2.1. The continuation

With $G = m = 1$ and the centre of mass at the origin, an orbit with the perpendicular start is mirror symmetric: it repeats after $2t$, rotated by an angle θ. For a given λ the unknowns (u_1, u_2, t) are fixed by three conditions on the state at t. With E the energy, L the angular momentum and $T = 2t$, the code uses $T^* = T|E|^{3/2}$, $L^* = |L||E|^{1/2}$ and turns $= \theta/2\pi$; T^* and L^* are closed forms of (u_1, u_2, λ, t). Hénon's relation between period and rotation along a family (Hénon, 1976, eq. 10) reads, in these units and in the frame of the code,

$$\mathrm{d}T^* = \pi L_s^* \mathrm{d}(\text{turns}), \tag{1}$$

with $L_s^* = L|E|^{1/2}$ keeping the sign of L.

The half orbit, of duration t, is cut into $m = 24$ pieces (multiple shooting). The unknowns are $z = (u_1, u_2, t, s_1, \ldots, s_{23})$, with s_i the state (12 numbers) at the start of piece $i+1$, so z has 279 components, 280 with λ. The equations are flow(s_i, t/m) $= s_{i+1}$ and the three closing conditions at the end of the last piece. Newton's method makes at most 12 iterations with a line search and stops when the largest absolute component of the equations is below 1e-11, the tolerance of the corrector.

The continuation is by pseudo-arclength in (z, λ) (Keller, 1977, 1987): the next point is sought on the hyperplane perpendicular to the tangent through the predicted point, so that folds, where a natural-parameter continuation (λ itself as the parameter) fails, can be passed. The arclength is the unscaled Euclidean norm over all 280 components; its step h, up to 0.2, is not a step in λ. A step is refused and halved if the corrector fails, if the tangent turns by more than 0.35 rad or if θ changes by more than $\max(0.03, 0.3|\theta|)$. After an accepted step h is multiplied by 1.4 if the corrector took at most 3 iterations, otherwise kept. If the step length falls below 1e-9 the trace stops.

2.2. The pieces and the regularised integrator

The end state of every piece comes from IAS15 (Rein and Spiegel, 2015) in REBOUND (Rein and Liu, 2012); the 12×12 matrix of a piece that is not an encounter piece comes from the variational equations of a Dormand–Prince code (Dormand and Prince, 1980). For an encounter piece the IAS15 end state is discarded; the end state and the matrix come from a regularised

integrator written for PeriCont, with algorithmic regularisation in chain coordinates (Mikkola and Tanikawa, 1999; the logarithmic Hamiltonian was introduced independently by Preto and Tremaine, 1999; chain: Mikkola and Aarseth, 1993). With chain vectors $Q_1 = r_b - r_a, Q_2 = r_c - r_b$, chain momenta $P_1 = -p_a, P_2 = -(p_a + p_b)$, kinetic energy $T(P) = \frac{1}{2} P^{\mathsf{T}} A P$ with A = [[2, −1], [−1, 2]] $\otimes\, I_2$, force function $U(Q) = \sum m_i m_j / |R_{ij}|$ and $B = -E$, the logarithmic Hamiltonian $\ln(T + B) - \ln U$ gives, in the fictitious time s,

$$Q' = (\partial T/\partial P)/(T + B), \quad P' = (\partial U/\partial Q)/U, \quad t' = 1/(T + B). \qquad (2)$$

A macro-step of the modified leapfrog uses 2, 4, 6, 8 sub-steps, is extrapolated in h^2 (Gragg, 1965; Bulirsch and Stoer, 1966) and is accepted if the error estimate is at most 1e-15. The physical time must end at exactly τ: when a macro-step would pass τ, the last step is found by Newton's method on $f(H) = t(H) - \tau$ in a bracket, to 4 units in the last place of the time increment.

The 12×12 matrix is the derivative of these operations, worked out by hand: each of the 12 unit perturbations of the Cartesian start is carried as a tangent through the drifts, the kicks and the extrapolation, and the dependence on the end time is removed by the correction $\delta Z - Z' \delta t / t'$ of the end state $Z = (Q, P)$, with $Z' = (AP/D,\ (\partial U/\partial Q)/U)$, $D = T(P) + B$ and $t' = 1/D$, also when the last macro-step lands exactly on τ (the end-time correction is derived in `docs/reg.md`; the tangents of the drifts and kicks, in `leapfrog`, and of the extrapolation, in `extrap` and `gbsStep`, are computed in `src/ias/reg.js` and not written out as formulae).

Three rules protect the pieces. An unflagged piece with a smallest IAS15 pair distance below 0.05 is also computed by the regularised integrator, which replaces IAS15 where the end states differ by 3e-12 or more (the cross-check). The regularised integrator also runs, without the matrix, on every other piece; a closest approach below 1e-3 found there counts as a missed flag, and below 5e-4 stops the trace. Four guards fail an attempt of the corrector when a third body comes near the close pair (second distance below 0.02, below 390 times the pericentre distance, or a node with a pair distance below 1e-4); after 5 failed attempts in a row with a trip the trace stops. These thresholds are chosen (Section 4.3).

2.3. Checks of stored points

A check integrates the stored (u_1, u_2, λ, t) of one point over a period in multiple precision (mpmath; an unregularised Gragg–Bulirsch–Stoer flow) with nothing of the program, in 40 digits (flow tolerance 1e-26) or 50 digits (1e-30). It gives the closure after the full period (best rotation removed) and the smallest pair distance, with a parabolic estimate between samples. A point counts as checked if the closure is below 1e-6, the energy and angular momentum change by less than 1e-14 (relative) and the minimum is in the range in which the flow was tested against the exact Kepler flow: 1e-7 or more for 40 digits, 1e-10 or more for 50 digits. The re-closer closes an orbit again at the same λ in 50 digits (Newton's method for (u_1, u_2, t) on the closing equations); the orbit is the same if (u_1, u_2, t) differ by 1e-9 relative or less. Check and re-closer use the same multiple-precision integrator, so they are independent of the program but not of each other.

3. What makes the difference

3.1. Ablation

The corrector was run with other integrators for the pieces on the two deepest stretches of the repository: t35 − from its replay start (31 recorded points, past its deepest step 10) and t44 − from its command-line start (40 recorded points, deepest step 34). Table 1 gives the result.

Table 1: The same corrector with other integrators for the pieces. "Passes" means that the run goes beyond the deepest step of the stored trace.

pieces by	t35 −	t44 −
default (regularised integrator for the encounter pieces, IAS15 for the others)	passes; 51 steps, 0 failed attempts, 336 s	passes; 57 steps, 1 failed, 816 s
regularised integrator for every piece	passes; 51 steps, 0 failed, 166 s; within 1.5e-11 of the default	passes; 57 steps, 1 failed, 241 s; within 1.0e-12
IAS15 for every piece, with the Dormand–Prince matrix	the start cannot be put on the family (6 numbers of pieces; with 64 pieces the run says that the start did not close)	6 steps, 30 failed; stops 2.4e-4 in λ from the start; the steps differ from the stored trace by up to 1.8e-2

pieces by	t35 −	t44 −
Dormand–Prince alone, tolerance 1e-9 and 1e-11	the start cannot be put on the family (residual 1.0e-7 to 2.8e-6)	24 pieces: not on the family; 8 pieces: 1 step at the first tolerance and 0 at the second, then 28 failed attempts
matrix of the regularised integrator by finite differences (forward, central)	10 and 5 of 31 points in 120 minutes	all 40 points; median 10 and 6 Newton iterations per step against 5

The regularised integrator is the part that makes the difference. With it for every piece the default result comes out at the same cost (the default took 162 s and 326 s when repeated beside it), and the orbit of the deepest step closes again in 50 digits within a relative 4e-14 and 1e-12 in (u_1, u_2, t). IAS15 stays the default away from an encounter because the stored traces were made with it; the cross-check overrules it on some pieces (Section 8, item 4). The row of IAS15 for every piece changes the end state and the matrix together, so the end states show the cause: IAS15 alone is off by 2.3e-3 to 2.2 against the 50-digit flow on the pieces with pair distances up to 1.6e-8, where the regularised integrator is within 5.5e-15.

Why Dormand–Prince fails. Through the accuracy of its end state on encounter pieces, not the tolerance: its failed attempts on t44 − (8 pieces) have best residuals 1.6e-9 to 5.0e-4 at the tolerance 1e-9 and 4.7e-10 to 7.5e-9 at 1e-11. None of the 15 runs of a different set takes an accepted step.

The matrix. With finite differences (as Hénon, 1974) the matrix of the four deepest encounter pieces is 276 (central) to 44765 (forward) times less accurate, and the corrector needs more iterations and fails more often (Table 1).

3.2. Cost

Table 2 gives the cost per unit of λ of PeriCont and of the natural-parameter continuation in 50 digits of the repository, counted the same way over the same stretch of λ: from accepted step 1, closed again in 50 digits, to the hand-over step k of Section 5.2 ($k = 262$ and 286). The 50-digit continuation takes fixed steps in λ, each from the secant of the two previous solutions: two steps of 7.5e-4 and one of 1.5e-3 for t35 −, two of 2e-3 and one of 4e-3 for t44 −. Every step converged; the cost is that of the larger

step, which covers the stretch in one step; larger steps were not tried, so it is an upper bound. PeriCont is the bit-for-bit replay of the stored trace to the step k (Section 10), run after the 50-digit jobs. Without bookkeeping, PeriCont is its corrector seconds over the accepted steps 1 to k and the 50-digit continuation the sum of its step seconds; for the whole run, both are wall time (PeriCont's with the recording of every accepted step, the 50-digit continuation's with the re-closing of the start).

Table 2: Seconds per unit of λ from accepted step 1 to the step k; ratio = 50-digit cost over PeriCont's. Wall-clock seconds, one job at a time. Total CPU load of the machine (median of the samples every minute): 37 % and 65 % (t35 −, t44 −) in the PeriCont replays and 66 % and 58 % in the 50-digit continuations, with two other processes of the machine, not started for these runs, using one core each throughout.

trace	PeriCont, corrector only	50 digits, steps only	ratio	PeriCont, whole replay	50 digits, whole runs	ratio
t35 − ($k = 262$)	3.3e5	1.0e5	0.32	4.0e5	1.7e5	0.42
t44 − ($k = 286$)	1.3e5	6.7e4	0.52	1.6e5	8.2e4	0.52

Counted the same way, PeriCont is not cheaper per unit of λ on these stretches: the 50-digit continuation costs 0.32 and 0.52 times as much without bookkeeping (the same per unit of arclength) and 0.42 and 0.52 times for the whole runs. With the smaller steps 3e-4 and 1e-3 of a first comparison, run with up to three jobs at a time, it cost 0.47 and 1.1 times as much over the whole stretch before the stall (accepted steps 1 to 1220 and 1 to 623). The same PeriCont steps took 574 s and 1307 s of corrector time in the stored runs, 468 s and 501 s in the replays here and 1049 s and 1821 s of wall time in the hand-over runs (Section 5.2); whether other jobs ran beside the stored runs is not recorded. The hand-over as measured passed the last λ of the stored traces after 1556 s and 2475 s, the 50-digit continuation alone after 255 s and 330 s. In the stall PeriCont costs at least 207 and 89 times as much per unit of λ as the 50-digit continuation at its untuned step of 1e-5 in λ, run beyond the stall.

3.3. What PeriCont gives that a 50-digit continuation does not

PeriCont gives a double-precision trace of many orbits: 0.43 and 0.43 accepted steps per second of wall time in the replays, against 0.0064 and 0.0037 converged orbits per second of the 50-digit continuation, at the steps

of Table 2 that set that rate; its orbits are closed in 50 digits, PeriCont's to the double-precision tolerance. It passes the close approaches, which IAS15 alone and Dormand–Prince alone do not (Table 1), and, as a pseudo-arclength continuation, folds in λ: t62 − and t72 − turn at $\lambda = 0.23310$ and 0.24076 in the runs of Section 4.3. It gives no lower cost per unit of λ on these stretches (Section 3.2). The 50-digit continuation of the repository is natural-parameter and cannot pass a fold in λ. On t14 + the 50-digit continuation, started from the re-closed orbit of the 25th accepted step, converges for 6 steps of 1.5e-4 in λ, the last 2.8e-5 below the first fold (at the 28th accepted step, $\lambda = 0.409904$), and the next step, 1.2e-4 above it, does not converge, while PeriCont passes the fold. A pseudo-arclength continuation in multiple precision, as Dena et al. (2012) describe, passes folds, and we did not test one; against it, neither the cost nor the passing of folds is a difference.

4. The families

4.1. Four families

19 starts were prepared; 15 were run and 4 were not, because a guard trips at the start orbit. Of the 15, 7 stopped by the triple-approach guard, 4 by leaving the region, 2 out of time and 2 by the step-length rule (t35 −, t44 − and t81 −: the stalls of Section 5).

Four traces reached checked distances below 1e-7: t35 −, t44 −, t62 − and t72 − (Table 3, Figure 2). None of their 854 checked points failed to close. The stretches are short: T^* changes by 0.05 % to 2.2 % and λ by 1.4e-3 to 3.6e-2.

Table 3: The four families. The checked distance is the minimum of the pair distance of the 50-digit flow, a parabolic estimate between samples (Section 2.3).

family	accepted steps	checked points	range of λ	change of T^* (%)	smallest checked distance (step)	largest closure of a checked point
t35 −	1711	69	1.4e-3	0.047	7.32e-10 (10)	9.8e-11
t44 −	1266	124	3.9e-3	0.46	1.91e-9 (34)	3.2e-9
t62 −	375	336	2.6e-2	2.2	8.57e-9 (9)	4.6e-9
t72 −	325	325	3.6e-2	1.9	1.61e-8 (97)	7.1e-9

The deepest values depend on where the steps landed: the re-closed midpoint of the steps 34 and 35 of t44 − has a checked distance of 1.34e-9, below its deepest step (1.91e-9); that of the steps 10 and 11 of t35 − is below the

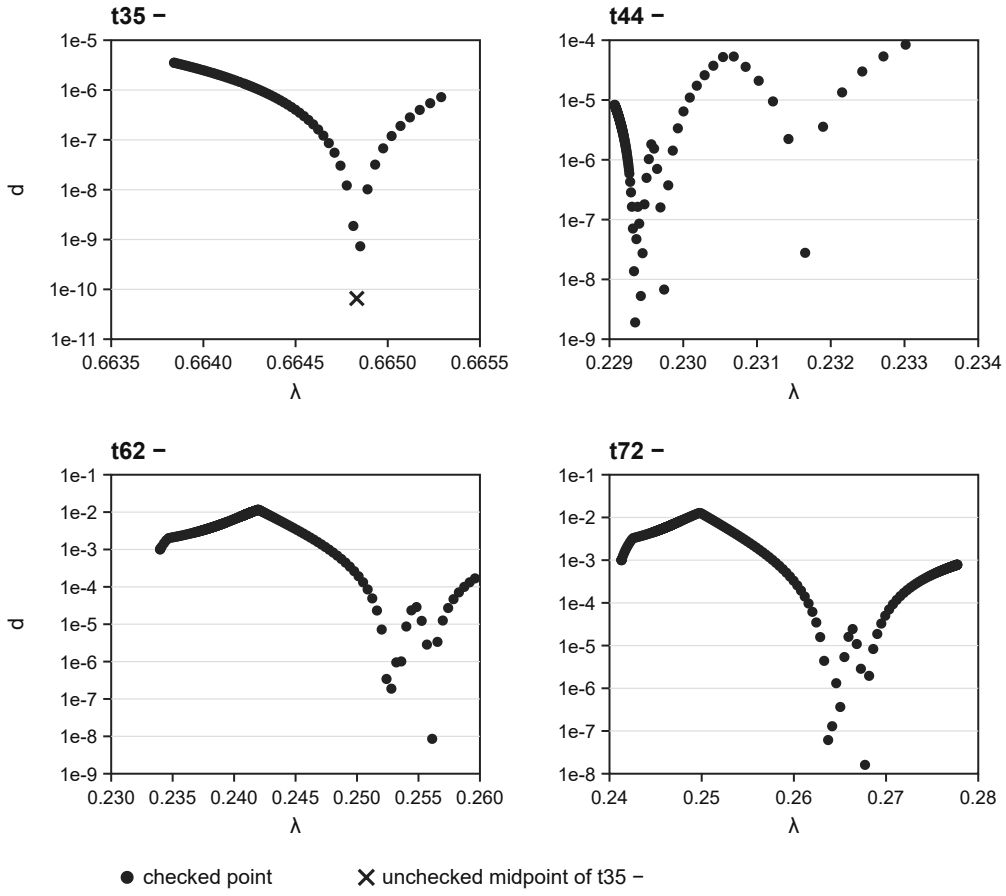


Figure 2: The checked minimum d of the pair distance against λ for the four families. Four minima of the t44 − panel, three between $\lambda = 0.2293$ and 0.2297 and one at 0.2317, are passages near collision orbits (Section 4.2); the cross in the t35 − panel is the re-closed midpoint below the range of the 50-digit flow, not checked.

1e-10 limit of the 50-digit flow and not checked; the smallest of the 10 midpoints of t62 − and t72 − near the deepest step are 73 and 25 times above their deepest steps.

4.2. Collision orbits

A family that passes through a collision orbit has a pair distance that goes to zero there while the angular momentum h of the close pair changes sign. Table 4 lists the 10 local minima of the checked distance below 1e-4 on the four traces. At the closest sample of the 50-digit flow, h changes sign next to 9 of them, always between two points with the same closest pair, and one re-closed midpoint brackets the λ of the collision orbit.

Table 4: Local minima of the checked distance and the bracket of λ in which h changes sign (the re-closed midpoints are in the data files).

family	step	checked distance	bracket of λ	width
t35 −	10	7.3e-10	0.66483212 to 0.66485085	1.9e-5
t44 −	34	1.9e-9	0.22933996 to 0.22934779	7.8e-6
t44 −	30	5.3e-9	0.22942473 to 0.22943654	1.2e-5
t44 −	21	6.8e-9	0.22971575 to 0.22974083	2.5e-5
t44 −	6	2.8e-8	0.23153976 to 0.23165305	1.1e-4
t62 −	17	1.9e-7	no sign change	–
t62 −	9	8.6e-9	0.25590018 to 0.25611411	2.1e-4
t72 −	106	6.1e-8	0.26393440 to 0.26415254	2.2e-4
t72 −	103	3.7e-7	0.26481296 to 0.26503401	2.2e-4
t72 −	97	1.6e-8	0.26771706 to 0.26794015	2.2e-4

For t35 − the square root of d is a V in λ (Figure 3). Over steps 1 to 25, d falls from 7.2e-7 to 7.3e-10 and rises to 5.6e-7. On each side of the minimum the six nearest checked points below 1e-7 lie on a line in the square root of d against λ with slopes 1.875 and −1.878, which cross zero at $\lambda_c = 0.66483640$ and 0.66483641. Each line reproduces its six points to a relative 5.5e-4 in d, and the end steps (steps 1 and 25) to 1.6e-3 and 1.6e-3 in the square root of d (3.2e-3 and 3.1e-3 in d). The data are consistent with a passage through, or very near, a collision orbit; the fitted λ_c lies inside the bracket of Table 4, and none was computed.

4.3. Beyond the guards

7 of the 15 traces stop at the triple-approach guard, among them t62 − and t72 −. Run from their last recorded point with the guards only recorded and not acted on, both go on until the limit of 60 minutes: 642 and 594 accepted steps, through a turn of λ at 0.23310 and 0.24076, to $\lambda = 0.396$

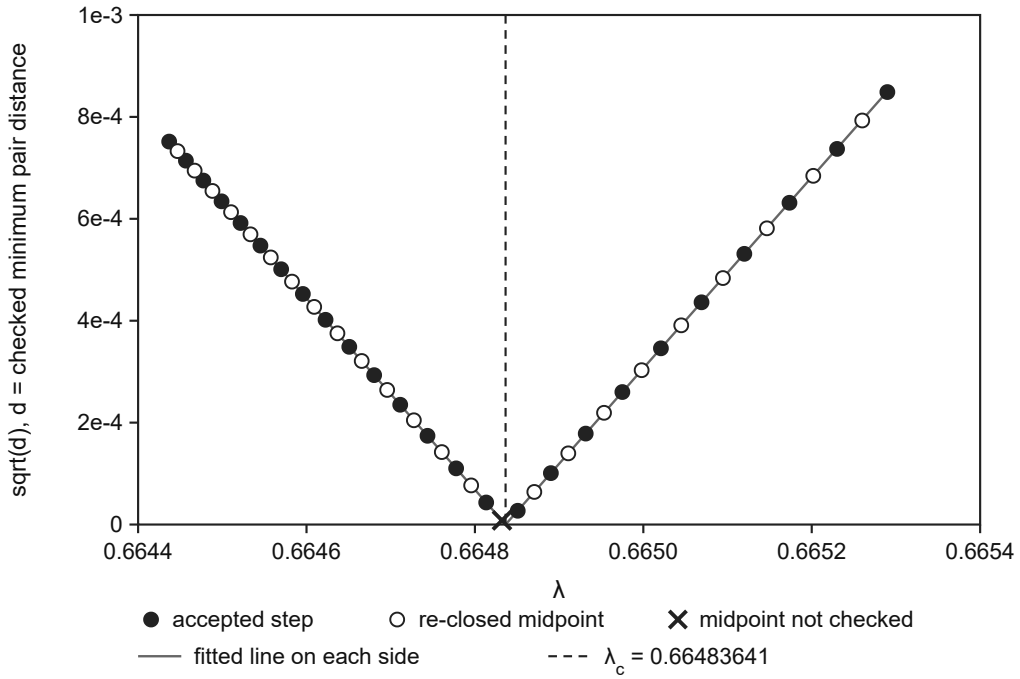


Figure 3: $\sqrt{d}$ against λ for the steps (filled) and re-closed midpoints (open) of t35 −, the two fitted lines, each extended from its six points to the steps 1 and 25, and the fitted λ_c (vertical line); the cross is the midpoint that is not checked.

and 0.396, where L^* has fallen to 0.019 and 0.020. The guards would have tripped 16355 and 10587 times, at ratios d_2/d_1 down to 5.8 and 5.6. The regularised integrator did not fail: there was no failure of it, no bridge error and no missed stop in either run. The corrector failed more often where the guards tripped: 82 of 520 attempts with a trip (16 %) against 3 of 207 without (1.4 %) on t62 −, 31 of 316 (9.8 %) against 3 of 312 (0.96 %) on t72 −; failed attempts are normal in a continuation, and the trips are not shown to be their cause. Five points of each run, evenly spaced over its recorded points, close again in 50 digits and are the same orbit to 1e-9; none is one of the 336 and 183 unrecorded accepted steps, and the first is at $\lambda = 0.272$ and 0.248, after 62 and 84 accepted steps, so the stretch from the turn to there has no re-closing. The run of t72 − counted 6 missed flags (a pair closer than 1e-3) and no missed stop. At the accepted, unrecorded step 32 of t72 − a trip of G2 had $d_1 = 1.1\text{e-}12$; its orbit re-closes to the same orbit (1e-12) and has a smallest pair distance of 7.4e-8, inside the range of the 50-digit check. Nothing is known nearer to a triple collision, where L^* goes to zero, and no piece of a tripped attempt was checked against the 50-digit flow as in Section 7.1.

5. The stall and the hand-over

5.1. The stall is a floor of the residual

Three traces stall: t35 − (from the 1221st accepted step), t44 − (from the 624th) and t81 − (from the 322nd). The boundary is a rule on the step in λ: a stall begins at the first accepted step from which every window of 100 consecutive accepted steps has a median step in λ of at most one hundredth of that of the first 500. The floor acts before it: of the failed attempts among the 500 attempts before the boundary, 128 of 128 (t35 −) and 41 of 43 (t44 −) end with a best residual between the tolerance and ten times it. Figure 4 shows the progress in λ. The median step in λ of the last 500 accepted steps is 6.7e-4 (t35 −), 1.0e-4 (t44 −) and 1.3e-7 (t81 −) of that of the first 500, and 82, 121 and 110 of them go backwards.

The cause is a floor of the residual in double precision, supported by Table 5, which says what it does not show. The corrector asks for a residual below 1e-11. Moving every node component by one unit in the last place changes the residual, at accepted steps in the stall of new runs with the tolerance raised to 1e-10 or 3e-10 beyond the last stored λ (not at stored steps, whose tolerance is 1e-11), by 7.2e-11 to 1.3e-10 (t44 −) and 5.1e-11

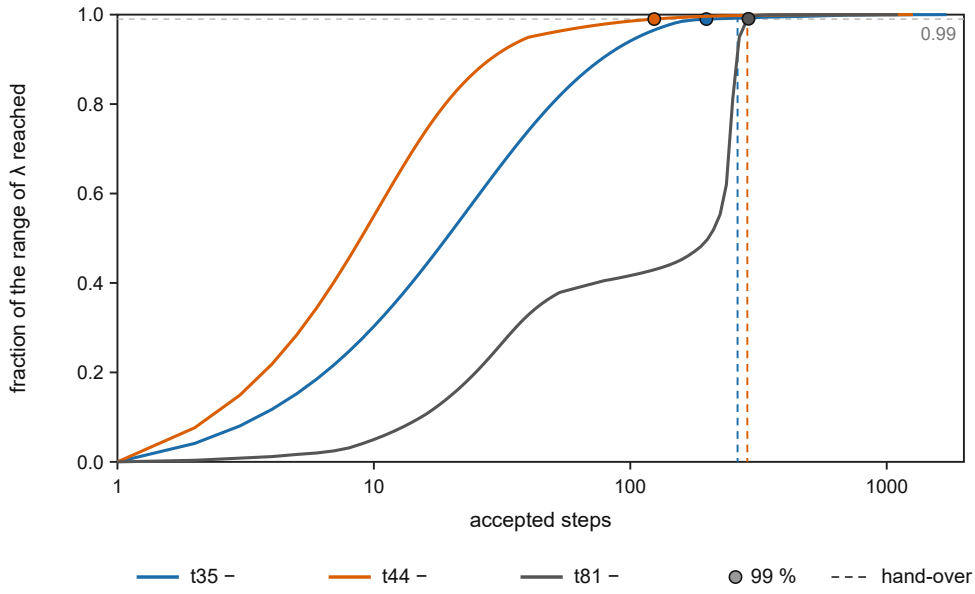


Figure 4: Fraction of the whole range of λ reached after the n-th accepted step, for t35 −, t44 − and t81 −. The vertical lines mark the hand-over of Section 5.2; the dots mark 99 %.

to 1.6e-10 (t35 −) (median of 30 trials), with the largest entry of the matrix of an encounter piece between 7e5 and 3e6; at four steps of t62 − without a stall (largest entry 59 to 137) the change is 1.8e-14 to 5.8e-14. In the stall the tolerance lies below the resolution of the residual, and an accepted step is reached by rounding luck: every failed attempt is a line search with a best residual just above the tolerance (209 of 209 of t35 − between 1.0e-11 and 3.5e-11).

Table 5: The evidence that the stall is a floor of the residual, and what it does not show.

test	result	does not show
tolerance raised to 1e-10, 30 minutes from the last stored step	t44 − goes 2.4e-6 and t35 − 1.6e-5 in λ beyond the stop, with 0 backward steps; with 1e-11 t44 − stops within 1.7e-7	that the points are on the family to 1e-10
five remedies (scaled tolerance, weighted arclength, natural-parameter steps, 48 pieces, two together)	none reaches 10 times the progress of the 1e-10 run (best 1.1 times); with the scaled tolerance 3 of 5 re-closed points of t44 − are not the 50-digit orbit at 1e-9	that no remedy exists
50-digit continuation beyond the stall	all 30 steps of −1e-5 converge for t35 −, t44 − and t81 −; the last orbits close to 8.2e-12 or better, at checked distances 4.3e-6, 1.6e-5 and 5.2e-4	steps beyond 1e-4

So the stall is a limit of the corrector and not an end of the family. The families go on at least 1e-4 in λ beyond the stalls (253 times the progress of t35 − over its last 500 accepted steps), as far as the 50-digit continuation shows; the second differences of the re-closed (u_1, u_2, t) of the 854 checked points along λ show no jump (largest ratio to the neighbours 3.0). In 50 digits the block $\mathrm{d}(r)/\mathrm{d}(u_1, u_2, t)$ of the closing Jacobian is regular at the stall points (ratio of smallest to largest singular value 1.3e-2 and 1.6e-3), so there is no fold or branch point.

5.2. The hand-over

The driver can stop the double-precision steps where the 50-digit continuation is faster and hand over to it. After at least 100 accepted steps, if the mean step in λ over the last 100 falls below 1e-7, the driver closes the last accepted point again in 50 digits and continues from it in steps of 1e-5. From the stored starts the rule fired after 262 and 286 accepted steps, where the stored traces had reached 99 % of their range at the 198th and 124th accepted step and began to stall at the 1221st and 624th. The double-precision parts

are bit for bit those of the stored traces. In the replays the median step in λ of an accepted step falls by a factor 383 (t35 −) and 226 (t44 −) from the accepted steps 1 to 50 to the steps 199 to 262 and 125 to 286. Mainly the λ component of the unit tangent falls (by 45 and 118; the step h in arclength is at most 0.2), and partly h itself (8.5 and 2.0): a failed attempt halves h, and it grows again only after a step of at most three iterations, which 6 of 64 and 1 of 162 of those last accepted steps are. The 6 failed attempts of t35 − after the accepted step 134 end with a best residual of 1.1e-11 to 2.4e-11, just above the tolerance. With the 50-digit continuation of Section 3.2 (9.5e-6 and 1.5e-5 in λ per second) and the wall seconds per accepted step of the replays (2.3 s and 2.3 s) the break-even P100 (the mean step in λ at which PeriCont makes as much λ per second) is 2.2e-5 for t35 − and 3.5e-5 for t44 −, 220 and 351 times the 1e-7 of the rule, which therefore hands over later than the break-even. The default is not changed in version 0.3.0. All 20 steps of the 50-digit continuation converged for both traces and went 1.9e-4 and 1.9e-4 beyond the last λ of the stored traces. The hand-over has a limit: at the collision end of family m (Section 6) the rule fires and the re-closing converges (the double-precision point is off by 2.4e-9, 2.9e-8 and 8.6e-8 in u_1, u_2, t), but the first 50-digit step, of 5e-6 in λ (`--handover-dlam`; the default is 1e-5), ended with a file-system error of the driver on Windows (fixed by retrying), and the retry did not converge in 10 updates (residual 3e-11); a smaller step was not tried.

6. Hénon's family m as an external benchmark

Hénon (1976, Table I) printed the orbits of the family m of equal masses to 8 decimals. PeriCont was run from his orbit 5, closed again in 50 digits, along the family with `--max-dist=inf` instead of the default 0.03 (as in the stored command; the family has no close approach over most of its length): 2462 recorded points from $\lambda = -0.9416$ to 0.99988. It passes his orbits 11, 28, 41 and 42 to 46. The orbit 11 is the zero of the rotation angle, found at $\lambda = -0.86525043$ against his -0.86525040. The orbits 28, 41, 42 and 46, closed again in 50 digits at his λ, agree with his converted values to 1.5e-8 or better, the level of his printed digits; the trace itself, interpolated at his λ, agrees with them to 2e-7 or better. The trace ends 1.2e-4 short of the collision orbit at $\lambda = 1$, where his table ends, by the stall of Section 5: all 24 pieces are encounter pieces and the closest approach is 1.2e-4.

7. Verification

7.1. The pieces

Table 6 compares the end states of the pieces with the 50-digit flow at the deepest checked step of each of the four families and at the last stored step of t44 −: every encounter piece, every piece replaced by the cross-check and the two neighbours of each (68 pieces). D is the largest of the 12 components of $|a-b|/\max(1,|b|)$. TRACE is REBOUND's close-encounter integrator (Lu, Hernandez and Rein, 2024); the table gives its best of three settings for each role.

Table 6: Largest D of an end state against the 50-digit flow, by integrator and role of the piece.

role (pieces)	IAS15 alone	regularised integrator	Dormand–Prince	TRACE
flagged (27)	2.2	2.4e-12	2.6e-6	34
cross-checked (6)	3.1e-14	2.3e-15	4.0e-12	0.15
neighbour (35)	5.6e-16	9.4e-16	1.4e-12	6.7e-6

The regularised integrator is within 2.4e-12 on every piece. IAS15 alone is off by up to 2.2 on the encounter pieces, the Dormand–Prince code gives up on 5 of them, and TRACE (three equal masses are outside its design; no matrix was compared) is off by up to 34.

7.2. What each check shows

Table 7 lists the checks.

Table 7: The checks, what each shows and what it does not show.

check	shows	does not show	result
regularised integrator against the exact Kepler flow	a pair's end state to a periapsis distance of 1e-10	a third body at close range; 1e-11	78 of 80 rows pass, 2 not graded
the same with a third body, against a 40-digit flow	no failure at the tested ratios of third-body to pair distance	smaller ratios (smallest tested 50)	all 44 rows pass

check	shows	does not show	result
the 12×12 matrix against a 60-digit reference (10 deepest encounter pieces), against double-precision central differences and against the exact Kepler matrix	the matrix to 2e-11 of its largest entry against the reference	the end states	1e-13 to 2e-11 against the reference, 1.1e-9 against the differences (their own accuracy), 4.3e-11 against the Kepler matrix, of $\max \lvert M \rvert$
the 50-digit flow against the exact Kepler flow	the flow to a pair distance of 1e-10	smaller distances	error 4.3e-20
the check and the re-closer at the same λ (854 stored points)	each point is near a closed orbit (within a relative 8.2e-11 of the re-closed one); its smallest pair distance	that consecutive points lie on one branch	largest closure 7e-9
Hénon's relation (1) between consecutive points	continuity before the stall	continuity in the stall	median deviation 2.0e-7 to 1.1e-6 on the four traces

Relation (1) was tested on the four traces by the rule of the repository's test (consecutive recorded points with |d(turns)| of 1e-6 or more): the medians of the relative deviation are 3.7e-7, 1.1e-6, 2.0e-7 and 3.0e-7 for t35 −, t44 −, t62 − and t72 −. It is largest for t44 − (above the 1e-6 of the repository's test) because its steps in turns are the smallest (median 6e-6): the deviation is dominated by an error of about 5e-12 in the turns, the level of the corrector tolerance.

8. Limitations and future work

1. **The path between two points rests on the regularised integrator.** The checks look at each point alone. Continuity was tested by re-closing along four stretches (64 values of λ, the stored orbits reproduced to 3e-12) and by the 50-digit continuation beyond the stall; Hénon's relation supports it before the stall only.
2. **A third body near the close pair is little tested.** The guards are chosen thresholds: 7 of the 15 traces stopped by a guard and 4 were not run because one trips at the start orbit. With the guards

only recorded, t62 − and t72 − go on (Section 4.3), so their stops are not shown to be failures of the method, but no piece of a tripped attempt was checked against the 50-digit flow as in Table 6, and near a triple collision nothing is checked: no tested ratio shows the regularised integrator failing, the smallest being 50, and the guards are tested on constructed states. The trace of t35 − had 3 trips of the guard G2, each of which failed one attempt.

3. **The cause of the stall is supported, not proven.** The hand-over passes it on the stretches tested; on family m it did not (Section 5.2).
4. **A check cannot check what the corrector solved.** The 279 components of an accepted step are stored by new runs only, so the stored traces have no node-by-node check. The cross-check covers pieces with a pair distance below 0.05 only, and its replacement logic has no test. On the stored traces of t35 −, t44 −, t62 − and t72 − it replaced the IAS15 end state 176, 3022, 10 and 2414 times. The regularised integrator for every piece costs no more (Table 1); IAS15 stays the default in 0.3.0 because the stored traces were made with it.
5. **One platform for the stored numbers** (Windows 11, Node.js v24.15.0, Python 3.14.6). On Ubuntu 24.04 the tests pass (Section 10) and a replay agrees to a relative 1e-11; the stored traces were not rerun there.

Future work. The stall should go with more precision in the residual at the nodes of the encounter pieces, or with regularised coordinates there; neither was tried. A multiple-precision pseudo-arclength continuation (Dena et al., 2012) would be the right baseline for the fold test and the cost.

9. Comparison with earlier work

Table 8 lists the works and their relation to PeriCont.

Table 8: Earlier work and its relation to PeriCont.

work	what it does	relation
Hénon (1974, 1976, 1977)	differential correction, Bulirsch–Stoer extrapolation, Waldvogel regularisation, matrix by finite increments; family m of equal masses; relation (1)	nearest older method (Sections 3.1, 6)
Wulff and Schebesch (2006, 2008); Wulff and Schilder (2009)	multiple shooting with tangential continuation; the rotating-Eight family through a close approach, unregularised, orbit scaled	no regularisation; pair distance not stated
Galán et al. (2002); Doedel et al. (2003); Muñoz-Almaraz et al. (2003, 2007)	boundary value software with first integrals and symmetries built in; the figure-eight continued in a mass; collisions reached, not passed	collocation with a regularised close pair, not tried
Dena et al. (2012); Abad, Barrio and Dena (2011); Abad et al. (2012)	pseudo-arclength continuation in multiple precision with a Taylor-series integrator; selected orbits corrected afterwards	established; no regularisation, relative periodic orbits or close approach in the pages read
Liao (2009); Li and Liao (2017); Hristov et al. (2024)	multiple-precision reruns and Newton refinement	the checks of Section 2.3 are of this kind, not validated
Mikkola and Tanikawa (1999); Mikkola and Aarseth (1993); Preto and Tremaine (1999); Mikkola and Innanen (1999); Trani et al. (2019); Mikkola and Merritt (2008); Rantala et al. (2020); Wang, Nitadori and Makino (2020)	algorithmic regularisation, the chain, the tangent map of a leapfrog map; few-body codes	the method of the regularised integrator; none describes the derivative of the extrapolated map at a fixed time
Lu, Hernandez and Rein (2024); Rein and Tamayo (2016); Capiński, Kepley and Mireles James (2023); Arioli and Mireles James (2025); Kapela and Simó (2007); Kapela et al. (2021)	TRACE and variational equations in REBOUND; rigorous work near collisions	TRACE is tested on the pieces (Table 6); the rigorous work is validated, the checks here are not

work	what it does	relation
Broucke (1975); Broucke and Boggs (1975); Hadjidemetriou (1975); Davoust and Broucke (1982); Schubart (1956); Waldvogel (1972); Aarseth and Zare (1974); Heggie (1974)	families of relative periodic orbits and their regularisation	none of the 130 typed orbits of Davoust and Broucke lies on the stretches within 1e-5; whether the families are among theirs is open
Šuvakov and Dmitrašinović (2013); Janković and Dmitrašinović (2016); Janković, Dmitrašinović and Šuvakov (2020); Chenciner and Montgomery (2000); Chenciner, Féjoz and Montgomery (2005)	catalogues from scans; satellites of Hénon's family; existence proofs	context

The four families are not satellites of Hénon's family m in the sense of Janković and Dmitrašinović (2016): the word of the syzygies of family m has the root 01 in all 40 orbits of Hénon's table for which it was computed, none of the 10 determined words of our 13 stretches has it, and none of the 57 entries of their Table I matches a stretch (best relative difference of T^* at equal L^* 0.63).

10. The program

Installation and tests. PeriCont is the route `integrator = 'ias'` of the repository, off unless asked for. It needs Node.js v24.15.0 and Python 3.14 with REBOUND 5.2.2, mpmath 1.4.1 and numpy 2.5.3 in a virtual environment, named by `ORBIT_PYTHON`; the commands for Windows (PowerShell, cmd) and Linux are in `docs/deep.md`. `npm test` runs the tests of the default route (46 PASS lines). `npm run test:ias` runs 14 test files of this route (135 PASS lines, 4 to 15 minutes), among them gate A, the matrices, the guards, the re-closer and the replay of a stored trace.

The settings that reproduce the paper. The stored runs used settings that differ from the defaults: the first step of IAS15 on a piece is REBOUND's 0.001 (`legacy`; the default sets it from the time scale of the pair), and the guard ratio is 400 for t35 − and t12 + (default 390). `tools/reproduce-trace.mjs LABEL OUT.json` builds the command of a stored trace from its

command-line start and these settings and compares the accepted steps with the stored ones. On the machine of the stored runs they agree bit for bit (not from the start in a trace file, which is moved onto the family again): all 325 accepted steps of t72 −, the first 23 of t62 −, 20 of t72 + and 20 of t81 −, and the first 262 and 286 of t35 − and t44 − in the hand-over runs.

The package, the sample run and the deposit. `node tools/pack-pericont.mjs OUTDIR` builds `pericont-0.3.0.zip` from `docs/pericont-files.txt`: 208 files, 2.0 MB. The numeric sample run `node tools/deep-sample.mjs` follows t35 − for 4 recorded points (25 accepted steps), checks all of them and compares numbers with tolerances; it takes 6 to 15 minutes. The second platform is the public run `https://github.com/Utshob-k/orbit-hunter/actions/runs/41312338787` of commit f877e5a of the release branch (the tag v0.3.0 adds only documentation and metadata to it), on Linux, where all tests pass: 46 and 135 PASS lines and no FAIL. The raw files behind `data/deep/extra` are deposited on Zenodo, `https://doi.org/10.5281/zenodo.23864862`.

Data availability

The code and the data of `data/deep` are in the repository and in the package (MIT licence for the code, CC BY 4.0 for the data and the text files). The raw files behind them are on Zenodo (`https://doi.org/10.5281/zenodo.23864862`), CC BY 4.0.

Appendix A. The files of PeriCont

`docs/pericont-files.txt` is the complete list.

- Integration and corrector: `src/ias/bridge.js`, `bridge-worker.mjs`, `ias-bridge.py`, `guards.py`, `recorder.js`, `reg.js`, `reg-settings.json`, and `src/shooting.js`, `perp.js`, `physics.js`, `stability.js`, `newton.js`, `relative.js`, `topology.js`, `settings.js`.
- Drivers: `tools/family-follow-ias.mjs`, `tools/reproduce-trace.mjs`, `tools/handover-rule.mjs`.
- Checks of stored points: `tools/witness.py`, `refine-mp.py`, `reclose.py`, `reclose-continue.py`, `trace-witnesses.py`, `witness-jobs.py`, `run-queue.py`, `kepler-ref.py`, `piece-ends.mjs`, `piece-mp.py`, `piece-trace.py`, `pair-angmom.py`, `residual-floor.mjs`.

- Package and sample: `tools/pack-pericont.mjs`, `tools/deep-sample.mjs`, `tools/paper-figures.py` (the four figures), `tools/cost-same-conditions.py` (Table 2), `cost-before-floor.py`, `step-limit.py`, `guards-record-checks.py` and `henon-relation.py` (Sections 3.2 to 5.2 and 7.2), which read the per-attempt records and run outputs of the deposit; the scripts that collated `cost-same-stretch.json` and `guards-record.json` are in the deposit only; `data/deep`, `docs/deep.md`, `docs/reg.md`.

- `reg.js` with `reg-settings.json` is self-contained and takes two or three bodies of any masses: `flowChain(masses, s, tau, { jac })` returns the end state at the time tau and, with `jac`, the derivative.

The rest of the repository (the WebGPU search, the satellites of the family R, the search tools of the Dormand–Prince route) is not needed for the route.

Declarations

Declaration of competing interest: The author declares no competing interests.

Funding: This research did not receive any specific grant from funding agencies in the public, commercial, or not-for-profit sectors.

CRediT authorship contribution statement: Utshob Kandel: Conceptualization, Methodology, Software, Validation, Formal analysis, Investigation, Data curation, Visualization, Writing – original draft, Writing – review & editing.

References

Aarseth, S.J., Zare, K., 1974. A regularization of the three-body problem. Celestial Mechanics 10, 185–205. doi:10.1007/bf01227619.

Abad, A., Barrio, R., Blesa, F., Rodríguez, M., 2012. Algorithm 924: TIDES, a Taylor series integrator for differential equations. ACM Transactions on Mathematical Software 39, Article 5. doi:10.1145/2382585.2382590.

Abad, A., Barrio, R., Dena, A., 2011. Computing periodic orbits with arbitrary precision. Physical Review E 84, 016701. doi:10.1103/PhysRevE.84.016701.

Arioli, G., Mireles James, J.D., 2025. Branches and bifurcations of ejection–collision orbits in the planar circular restricted three body problem. Nonlinearity 38, 045010. doi:10.1088/1361-6544/adbda3.

Broucke, R., 1975. On relative periodic solutions of the planar general three-body problem. Celestial Mechanics 12, 439–462. doi:10.1007/bf01595390.

Broucke, R., Boggs, D., 1975. Periodic orbits in the planar general three-body problem. Celestial Mechanics 11, 13–38. doi:10.1007/bf01228732.

Bulirsch, R., Stoer, J., 1966. Numerical treatment of ordinary differential equations by extrapolation methods. Numerische Mathematik 8, 1–13. doi:10.1007/bf02165234.

Capiński, M.J., Kepley, S., Mireles James, J.D., 2023. Computer assisted proofs for transverse collision and near collision orbits in the restricted three body problem. Journal of Differential Equations 366, 132–191. doi:10.1016/j.jde.2023.03.053.

Chenciner, A., Féjoz, J., Montgomery, R., 2005. Rotating eights: I. The three Γ_i families. Nonlinearity 18, 1407–1424. doi:10.1088/0951-7715/18/3/024.

Chenciner, A., Montgomery, R., 2000. A remarkable periodic solution of the three-body problem in the case of equal masses. Annals of Mathematics 152, 881–901. doi:10.2307/2661357.

Davoust, E., Broucke, R., 1982. A manifold of periodic orbits in the planar general three-body problem with equal masses. Astronomy and Astrophysics 112, 305–320.

Dena, A., Rodríguez, M., Serrano, S., Barrio, R., 2012. High-precision continuation of periodic orbits. Abstract and Applied Analysis 2012, Article ID 716024. doi:10.1155/2012/716024.

Doedel, E.J., Paffenroth, R.C., Keller, H.B., Dichmann, D.J., Galán-Vioque, J., Vanderbauwhede, A., 2003. Computation of periodic solutions of conservative systems with application to the 3-body problem. International Journal of Bifurcation and Chaos 13, 1353–1381. doi:10.1142/s0218127403007291.

Dormand, J.R., Prince, P.J., 1980. A family of embedded Runge–Kutta formulae. Journal of Computational and Applied Mathematics 6, 19–26. doi:10.1016/0771-050X(80)90013-3.

Galán, J., Muñoz-Almaraz, F.J., Freire, E., Doedel, E., Vanderbauwhede, A., 2002. Stability and bifurcations of the figure-8 solution of the three-body problem. Physical Review Letters 88, 241101. doi:10.1103/PhysRevLett.88.241101.

Gragg, W.B., 1965. On extrapolation algorithms for ordinary initial value problems. Journal of the Society for Industrial and Applied Mathematics, Series B: Numerical Analysis 2, 384–403. doi:10.1137/0702030.

Hadjidemetriou, J.D., 1975. The continuation of periodic orbits from the restricted to the general three-body problem. Celestial Mechanics 12, 155–174. doi:10.1007/BF01230209.

Heggie, D.C., 1974. A global regularisation of the gravitational N-body problem. Celestial Mechanics 10, 217–241. doi:10.1007/bf01227621.

Hénon, M., 1974. Families of periodic orbits in the three-body problem. Celestial Mechanics 10, 375–388. doi:10.1007/BF01586865.

Hénon, M., 1976. A family of periodic solutions of the planar three-body problem, and their stability. Celestial Mechanics 13, 267–285. doi:10.1007/BF01228647.

Hénon, M., 1977. A relation in families of periodic solutions. Celestial Mechanics 15, 99–105. doi:10.1007/BF01229050.

Hristov, I., Hristova, R., Dmitrašinović, V., Tanikawa, K., 2024. Three-body periodic collisionless equal-mass free-fall orbits revisited. Celestial Mechanics and Dynamical Astronomy 136, 7. doi:10.1007/s10569-023-10177-w.

Janković, M.R., Dmitrašinović, V., 2016. Angular momentum and topological dependence of Kepler's third law in the Broucke–Hadjidemetriou–Hénon family of periodic three-body orbits. Physical Review Letters 116, 064301. doi:10.1103/PhysRevLett.116.064301.

Janković, M.R., Dmitrašinović, V., Šuvakov, M., 2020. A guide to hunting periodic three-body orbits with non-vanishing angular momentum. Computer Physics Communications 250, 107052. doi:10.1016/j.cpc.2019.107052.

Johansson, F., the mpmath development team, 2026. mpmath: a Python library for arbitrary-precision floating-point arithmetic. URL: https://mpmath.org/. version 1.4.1.

Kapela, T., Mrozek, M., Wilczak, D., Zgliczyński, P., 2021. CAPD::DynSys: a flexible C++ toolbox for rigorous numerical analysis of dynamical systems. Communications in Nonlinear Science and Numerical Simulation 101, 105578. doi:10.1016/j.cnsns.2020.105578.

Kapela, T., Simó, C., 2007. Computer assisted proofs for nonsymmetric planar choreographies and for stability of the Eight. Nonlinearity 20, 1241–1255. doi:10.1088/0951-7715/20/5/010.

Keller, H.B., 1977. Numerical solution of bifurcation and nonlinear eigenvalue problems, in: Rabinowitz, P.H. (Ed.), Applications of Bifurcation Theory. Academic Press, New York, pp. 359–384.

Keller, H.B., 1987. Lectures on Numerical Methods in Bifurcation Problems. Tata Institute of Fundamental Research, Bombay, and Springer, Berlin.

Li, X., Liao, S., 2017. More than six hundred new families of Newtonian periodic planar collisionless three-body orbits. Science China Physics, Mechanics & Astronomy 60, 129511. doi:10.1007/s11433-017-9078-5.

Liao, S., 2009. On the reliability of computed chaotic solutions of non-linear differential equations. Tellus A 61, 550–564. doi:10.1111/j.1600-0870.2009.00402.x.

Lu, T., Hernandez, D.M., Rein, H., 2024. TRACE: a code for time-reversible astrophysical close encounters. Monthly Notices of the Royal Astronomical Society 533, 3708–3723. doi:10.1093/mnras/stae1982.

Mikkola, S., Aarseth, S.J., 1993. An implementation of N-body chain regularization. Celestial Mechanics and Dynamical Astronomy 57, 439–459. doi:10.1007/bf00695714.

Mikkola, S., Innanen, K., 1999. Symplectic tangent map for planetary motions. Celestial Mechanics and Dynamical Astronomy 74, 59–67. doi:10.1023/a:1008312912468.

Mikkola, S., Merritt, D., 2008. Implementing few-body algorithmic regularization with post-Newtonian terms. The Astronomical Journal 135, 2398–2405. doi:10.1088/0004-6256/135/6/2398.

Mikkola, S., Tanikawa, K., 1999. Algorithmic regularization of the few-body problem. Monthly Notices of the Royal Astronomical Society 310, 745–749. doi:10.1046/j.1365-8711.1999.02982.x.

Muñoz-Almaraz, F.J., Freire, E., Galán, J., Doedel, E., Vanderbauwhede, A., 2003. Continuation of periodic orbits in conservative and Hamiltonian systems. Physica D: Nonlinear Phenomena 181, 1–38. doi:10.1016/s0167-2789(03)00097-6.

Muñoz-Almaraz, F.J., Freire, E., Galán-Vioque, J., Vanderbauwhede, A., 2007. Continuation of normal doubly symmetric orbits in conservative reversible systems. Celestial Mechanics and Dynamical Astronomy 97, 17–47. doi:10.1007/s10569-006-9048-3.

Preto, M., Tremaine, S., 1999. A class of symplectic integrators with adaptive time step for separable Hamiltonian systems. The Astronomical Journal 118, 2532–2541. doi:10.1086/301102.

Rantala, A., Pihajoki, P., Mannerkoski, M., Johansson, P.H., Naab, T., 2020. MSTAR – a fast parallelized algorithmically regularized integrator with minimum spanning tree coordinates. Monthly Notices of the Royal Astronomical Society 492, 4131–4148. doi:10.1093/mnras/staa084.

Rein, H., Liu, S.F., 2012. REBOUND: an open-source multi-purpose N-body code for collisional dynamics. Astronomy and Astrophysics 537, A128. doi:10.1051/0004-6361/201118085.

Rein, H., Spiegel, D.S., 2015. IAS15: a fast, adaptive, high-order integrator for gravitational dynamics, accurate to machine precision over a billion orbits. Monthly Notices of the Royal Astronomical Society 446, 1424–1437. doi:10.1093/mnras/stu2164.

Rein, H., Tamayo, D., 2016. Second-order variational equations for N-body simulations. Monthly Notices of the Royal Astronomical Society 459, 2275–2285. doi:10.1093/mnras/stw644.

Schubart, J., 1956. Numerische Aufsuchung periodischer Lösungen im Dreikörperproblem. Astronomische Nachrichten 283, 17–22. doi:10.1002/asna.19562830105.

Šuvakov, M., Dmitrašinović, V., 2013. Three classes of Newtonian three-body planar periodic orbits. Physical Review Letters 110, 114301. doi:10.1103/PhysRevLett.110.114301.

Trani, A.A., Spera, M., Leigh, N.W.C., Fujii, M.S., 2019. The Keplerian three-body encounter. II. Comparisons with isolated encounters and impact on gravitational wave merger timescales. The Astrophysical Journal 885, 135. doi:10.3847/1538-4357/ab480a.

Waldvogel, J., 1972. A new regularization of the planar problem of three bodies. Celestial Mechanics 6, 221–231. doi:10.1007/bf01227784.

Wang, L., Nitadori, K., Makino, J., 2020. A slow-down time-transformed symplectic integrator for solving the few-body problem. Monthly Notices of the Royal Astronomical Society 493, 3398–3411. doi:10.1093/mnras/staa480.

Wulff, C., Schebesch, A., 2006. Numerical continuation of symmetric periodic orbits. SIAM Journal on Applied Dynamical Systems 5, 435–475. doi:10.1137/050637170.

Wulff, C., Schebesch, A., 2008. Numerical continuation of Hamiltonian relative periodic orbits. Journal of Nonlinear Science 18, 343–390. doi:10.1007/s00332-008-9026-x.

Wulff, C., Schilder, F., 2009. Numerical bifurcation of Hamiltonian relative periodic orbits. SIAM Journal on Applied Dynamical Systems 8, 931–966. doi:10.1137/080733267.